Application of Advanced CFD Technology to Energy-Saving Hull form Development

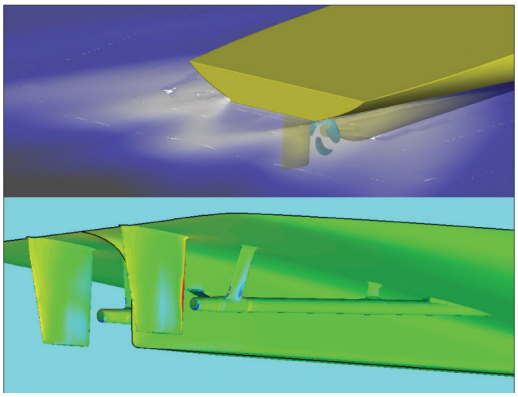

MAKOTO NISHIGAKI*1 MAKOTO KAWABUCHI*2

SATORU ISHIKAWA*3

Due to the advancement of computational fluid dynamics (CFD) technology, CFD can cope with many cases of hull form development. Mitsubishi Heavy Industries, Ltd. (MHI) evaluates hull resistance and propulsive efficiency using the most of the latest CFD technology, which can be robustly applied to wave-making computation in consideration of free surface against complex forms of hulls and appendages, as well as propeller-considered self-propulsion computation at a high degree of accuracy and speed, while deriving refinements for forms of hulls and appendages from information such as the circumstances of waves created by the hull and flow around the hull. We will continue to use such technologies to further improve the energy-saving performance of vessels.

1. Introduction

While CFD technology is making remarkable progress, in a bid to be effectively applied to developing energy-saving hull forms, it is an important factor, as well as to have an estimated accuracy sufficient to derive refinements, to be able to quickly generate grids so that performance can be evaluated for complex forms of actual ships, to be able to robustly correspond to analyses including free surface and to be able to perform large-scale grid and numerous computations at a high speed. Using the latest CFD software and large-scale parallel computers that meet these goals, MHI is performing wave-making and self-propulsion computations to promote energy-saving hull form development, which is introduced in this report with examples.

2. Computing method

2.1 Wave-making computation

Optimization in the shape of stern edge is essential for the development of energy-saving hull forms, as it seriously affects the properties of stern wave-making and consequently the ship's propulsive performance. With the existing CFD method for free surface flow using structured grids and the surface tracking method, in which grids are transformed in accordance with changes in the water surface, CFD was not fully used to actually design the stern edge form, since the expert knowledge/time required for grid generation as well as the robustness of the computation was limited As a result, MHI has been shifting to unstructured grids and the surface capturing method, in which grids are fixed and free surface analysis uses a density function, with the aim of establishing a more robust computing method. As unstructured hexahedral grid technology advanced, it is now likely that high-quality grids can be generated in a short time, even for complex geometries. As for the surface capturing method, it is also likely that robust wave patterns can be acquired at a high degree of accuracy as multi-purpose CFD code technology advanced.

Previously, the number of grids has been limited due to computing capability, resulting in

*1 Chief Staff Manager, Nagasaki Research & Development Center, Technology & Innovation Headquarters
*2 Nagasaki Research & Development Center, Technology & Innovation Headquarters
*3 Senior Manager, Nagasaki Research & Development Center, Technology & Innovation Headquarters

rough grids in areas distant from the hull and dense grids only in areas close to the hull, and we have been striving to reduce wave-making resistance caused by the divergence wave (八-shaped wave) splitting from the bow, setting the wave profiles as a major evaluation index. However, to perform more accurate computing, it is desirable to expand the range of grid fragmentation, and when reviewing the stern form in particular, we expanded the range of grid fragmentation around the free surface in the rear part of the hull as well, as the state of transverse waves there will also matter. Because the automatic mesh generator is used to generate unstructured grid, factors such as the number of grids in the corresponding parts are not fully fixed between the two hull forms being compared, unlike in the structured grid. To prevent grids from affecting computing results, the number of grid compartments has to be increased more than in the structured grid.

Considering these factors, the number of grids was increased from the previous hundreds of thousands level to the million to tens of millions level. **Table 1** shows a comparison of the existing CFD and the latest CFD computing methods, while **Figure 1** shows an example of computed grid comparisons around the stern and **Figure 2** shows a comparison of computing results. It can be seen that the latest CFD can capture a broad range of wave-making circumstances, while truly reflecting the stern form and sharply increasing the number of grids.

Table 1 Comparison of previous CFD and latest CFD methods

	Previous CFD	Latest CFD
Treatment of stern shape	Modified or simplified to ensure stable computing	Complex geometry truly accounted for
Grid type	Structured grid	Unstructured hexahedral grid
Treatment of free surface in wave-making computation	Surface tracking method [1)]	Surface capturing method [2)] (VOF [3)])
Grid number	Hundreds of thousands	Millions to tens of millions
Propeller model in self-propulsion computing	Body force model by UQCM [4)]	Body force model by UQCM [4)]
Turbulence model	SR222 revised Baldwin Lomax model (0 equation)	SST k-ω (2 equation)
Number of CPUs used in parallel computing	1	16-64

1) Method that transforms grids in accordance with changes in free surface
2) Surface capturing method: A method to analyze free surface by density functions using fixed grids
3) VOF: Volume of Fluid
4) UQCM: Unsteady Quasi-Continuous Method

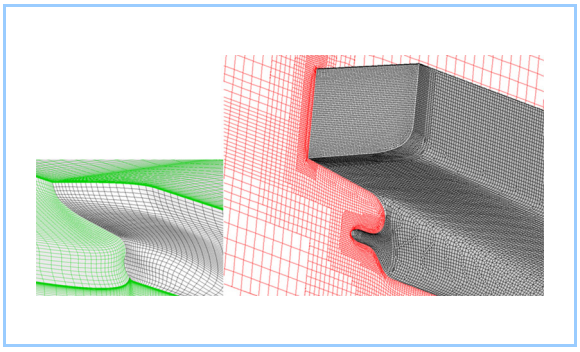

Figure 1 Comparison of wave-making computation grid using previous CFD (left) and latest CFD (right) (RoRo vessel)
While the transom was extended and the stern tube was curled to ensure computing stability with the previous CFD using a structured grid, stern geometry is truly reflected and the number of grids is greatly increased with the latest CFD using unstructured hexahedral grids.

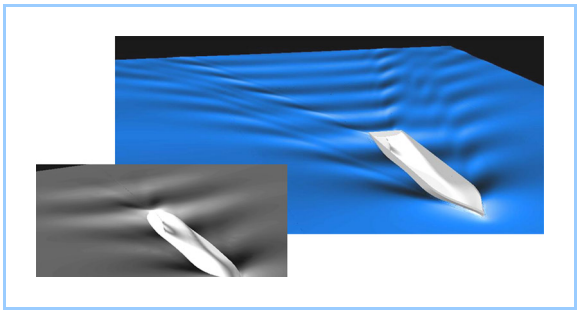

Figure 2 Comparison of wave-making computation results by previous CFD (left) and latest CFD (right) (KRISO container ship)
The latest CFD captures the wave extending obliquely backward from the bow and the stern in a wide range.

Figure 3 shows an example of comparisons between an experiment and the wave pattern computing results using the latest CFD, in which the positions and heights of longitudinal and transverse waves were mostly in agreement between the experiment and CFD.

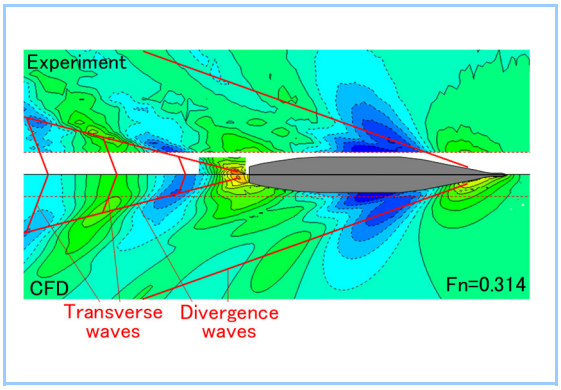

Figure 3 Comparison of wave pattern experiment and CFD (ferry)
Red and blue represent high and low wave heights, respectively, in this contour map. Position and height of divergence waves and transverse waves are largely in agreement between experiment and CFD.

Figure 4 shows a comparison of local wave-making circumstances near the stern with a photo. The form of wave-making captured by CFD agrees with the experiment result on the side edges at the end of the stern.

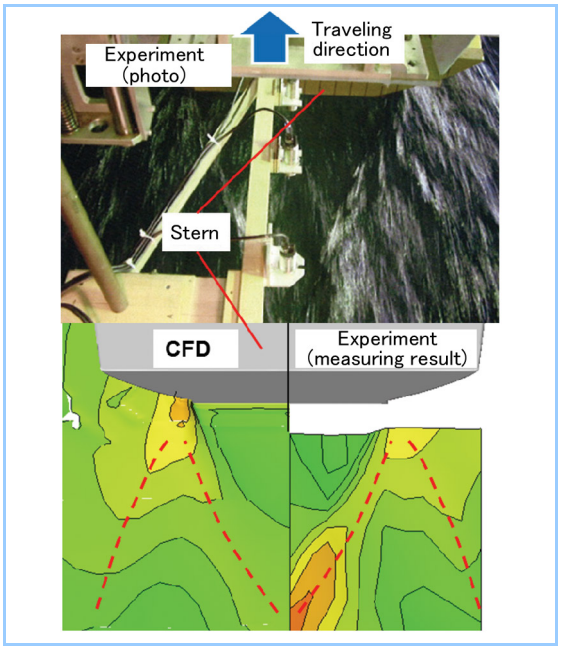

Figure 4 Comparison with experiment photo of wave-making around stern (ferry)
This shows a comparison of CFD (bottom left) and model experiment (top: photo, bottom right: measuring result) of the local wave circumstances behind the stern of a ferry.
The form of waves extending obliquely backward from both corners of the stern agrees in CFD and experiment (red dot-lines in figures below), which looks white in the experiment photo.

2.2 Self-propulsion computing

MHI has evaluated the effect of propeller inlet flow by incorporating the UQCM (Unsteady Quasi-Continuous Method) propeller computing method as a body force propeller model. We performed self-propulsion computing by incorporating the same method with the multi-purpose CFD code.

In addition, we performed this self-propulsion computing without taking free surface into consideration (in symmetrical condition) due to issues concerning the stability and computing time. So, computed grids are different from those created by wave-making computation. Like wave-making computation, however, we used an unstructured hexahedral grid and truly reflected the complex geometries in front of and behind the propeller. As developed boundary-layer flow enters the spaces in front of and behind the propeller, we tried to increase the accuracy by increasing the grid density higher than usual in these areas. The number of grids reached the millions, one order larger than in other areas, by parallel computing using multi-purpose codes.

Figure 5 shows the estimate accuracy of self-propulsion factors (t: thrust deduction coefficient and wm: wake fraction) computed by the aforementioned self-propulsion computing method. Challenges remain in the estimate accuracy, with the wm computed by CFD generally indicating lower figures than those acquired from basin experiments, for example. Accordingly, we are currently estimating self-propulsion performance by always comparing CFD results with experimental results. We will continue to improve the method and leverage the results for improving a stern form that boasts superior self-propulsion performance.

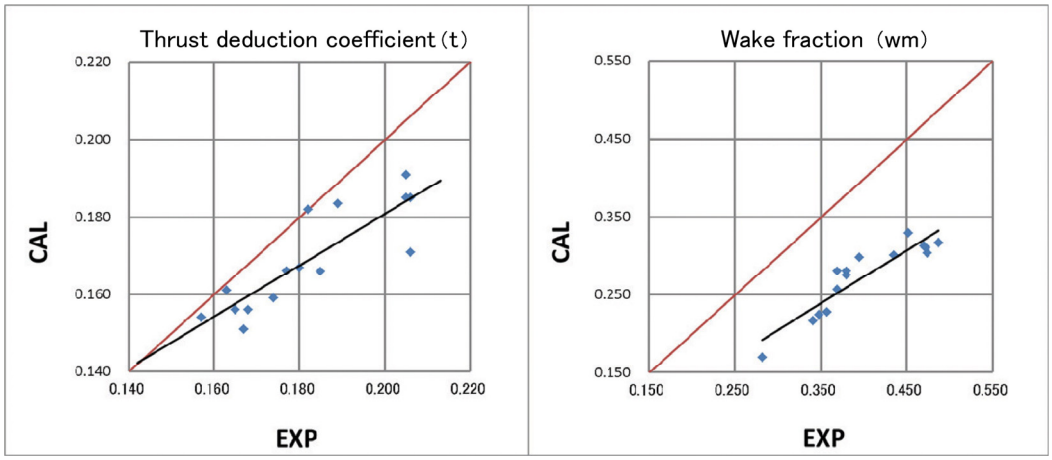

Figure 5 Estimate accuracy of self-propulsion computing using body force propeller model
The thrust deduction coefficient (t) and wake fraction (wm), which are self-propulsive factors, exhibit good mutuality between the experiment and CFD. Given a few challenges including the smaller wm evaluation than in the experiment, estimation is always carried out in comparison with experimental results.

3. Computing examples

To develop energy-saving hull forms using the computing method mentioned above, analysis of the flow around the hull is very important. In this section, we will explain the accuracy of flow evaluation using three examples, namely the review of improvement in the stern edge shape using the stern wave height evaluation, flow field evaluation for twin-skeg hull forms and flow field evaluation of the propeller plane behind the shaft bracket, all of which have been difficult using existing CFD computing.

3.1 Evaluation of stern wave pattern

Figure 6 is a contour map of a wave pattern by CFD computing for the hull of a high-speed ship before and after improving the stern edge shape. As a result of hull form improvement, waves were lowered immediately behind the stern edge and posterior. **Figure 7** shows a comparison of residual resistance in the experiment and CFD computation on these two hull forms, which exhibit the accuracy of CFD computing showing that the hull form improvement resulted in lower residual resistance.

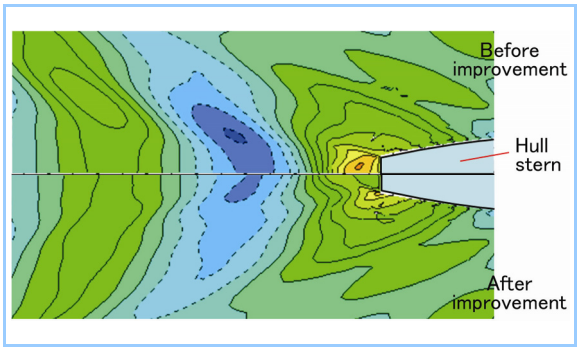

Figure 6 CFD comparison of stern wave heights before and after improvement in stern edge shape (ferry)
This shows that the wave heights behind the stern are lowered as a result of the improvement in the stern edge shape.

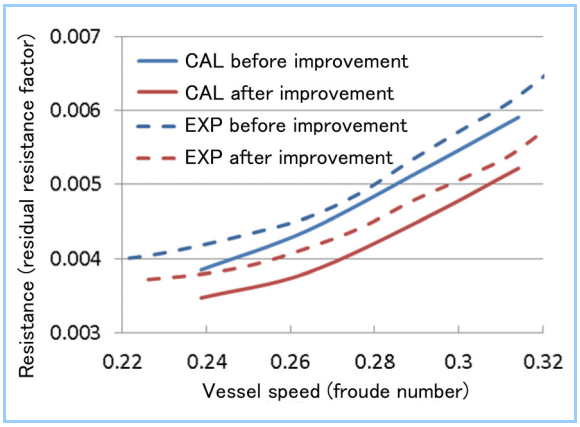

Figure 7 Resistance reduced by different stern edge shapes (ferry)
This shows CFD also captures resistance reduced in a broad range by improvements in the shape of the stern edge.

3.2 Evaluation of flow field of twin-skeg hull form

When developing a twin-skeg hull form as shown in **Figure 8**, evaluating the asymmetric nature of the flow field inside and outside of the skegs becomes important. Shown in the same Figure 8 is a comparison of flow lines between the skegs acquired by paint testing and CFD computing, and the position and forms of the flow separation line, which can be observed in both results, are similar to each other.

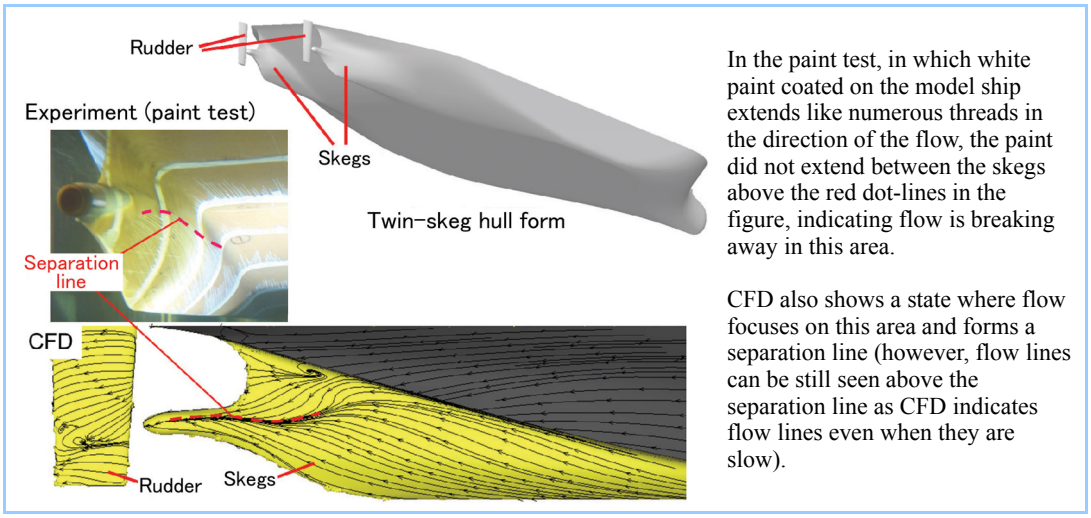

Figure 8 Twin-skeg Hull Form and Flow between Skegs

Figure 9 shows a comparison of the flow field on the propeller plane on the port side. A strong upflow can be confirmed between the skegs, while inward flow from outer side is generated down below, making the wake at the bottom edge of the skegs flow inward. CFD also captured these characteristic flow trends. In this manner, CFD computing can efficiently evaluate flow field circumstances in detail, even when it is such a complex stern form such as a twin-skeg, and lead to further hull form improvement using this flow field information as a reference.

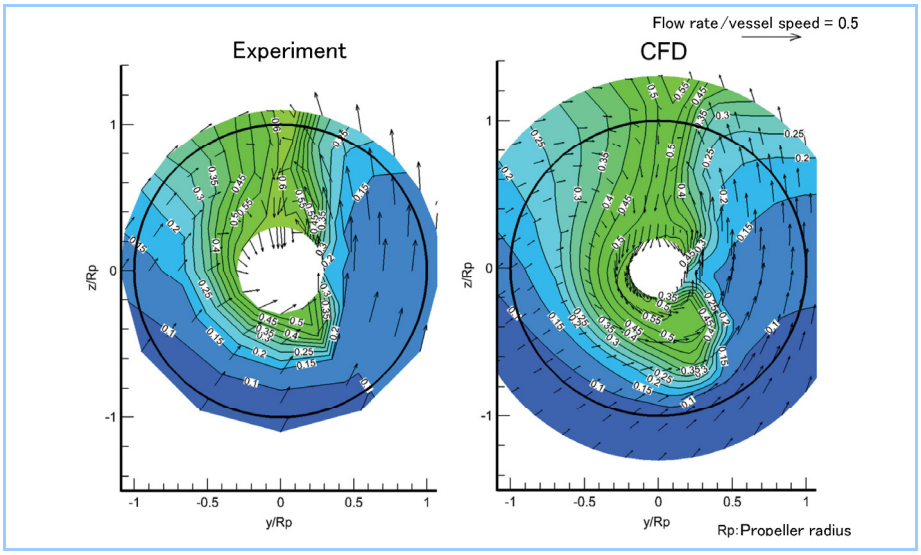

Figure 9 Flow field on propeller plane of twin-skeg hull (left propeller)
The bluer the contour map is, the faster the relative flow rate is against the hull. The upflow strengthens between the skegs. Inward flow from outer side down below is making the slow zone behind the skeg flow inward. CFD captures these circumstances as well.

3.3 Evaluation of flow field on propeller plane behind shaft brackets

Figure 10 shows the pressure pattern of a hull form embedded with shaft brackets and the propeller plane flow field behind the shaft brackets. In the flow field on the propeller plane, a total of three wakes including that of shaft itself between the wakes of the two brackets can be seen, and this property of the flow field is captured by CFD computing.

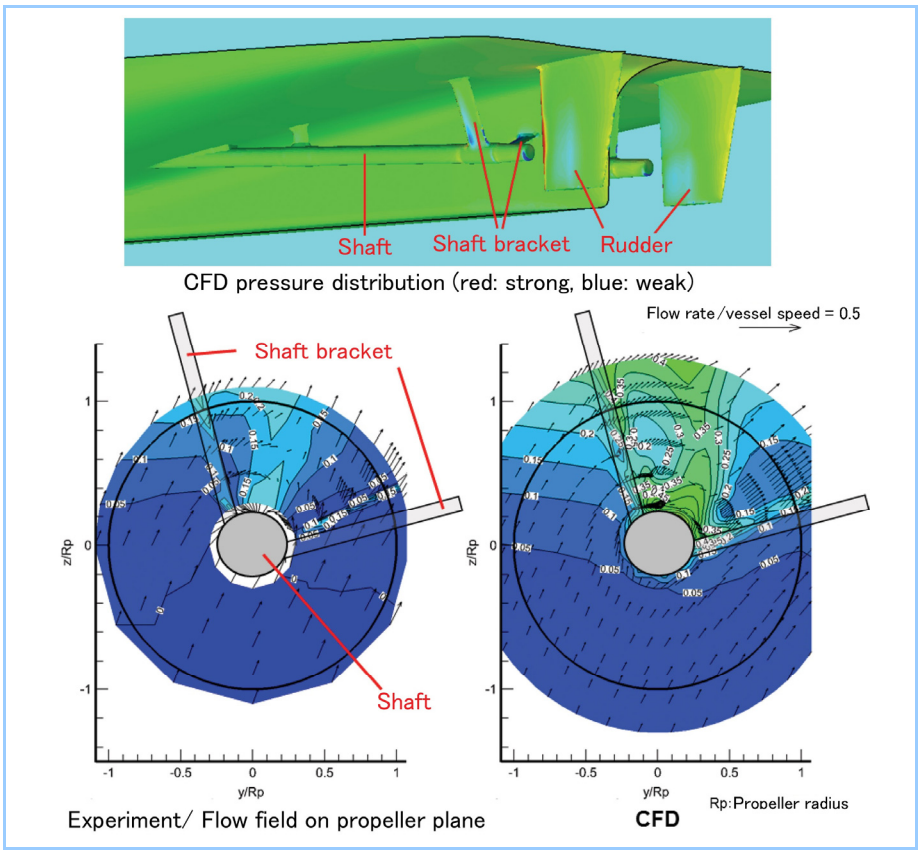

Figure 10 Shaft bracket-embedded hull form's pressure pattern and flow field on propeller plane (left propeller)

A total of three relatively slow zones are generated in the lower course of the shaft itself and two brackets by upward and inward flow seen in the flow field vectors on the propeller planes, which is also captured by CFD.

4. Conclusion

MHI established a practical CFD method that can evaluate the effect of a complex hull form near the stern or appendages on a ship's performance and flow fields, which are significant factors when developing an energy-saving vessel, by using the latest CFD technology capable of large scale unstructured grids (hexahedral grids) on a scale of millions to tens of millions, as well as robust free surface analyses and high-speed computing based on parallel computers. We are improving the energy-saving performance by applying this method to evaluating wave patterns, the flow field of the twin-skeg hull form and the propeller plane flow field behind the shaft bracket, etc,, which have been difficult to evaluate, in order to derive refinements from the flow field information. From now on, MHI will continue to establish a design method considering scale effect and ship resistance waves, focusing on ship performance in actual seas.

Reference

1. Takada et al., Journal of The Japan Institute of Marine Engineering No. 197 (2002) p.63